



# Radiative exchange in a parallel-plate enclosure with translucent protective coatings on its walls

Robert Siegel\*

Research and Technology Directorate, NASA Lewis Research Center, Cleveland, OH 44135, U.S.A.

Received 7 January 1998; in final form 5 April 1998

---

## Abstract

Thermal barrier and protective coatings are used for reducing temperatures in metal walls in high temperature applications, and for protection in corrosive environments. Radiative transfer is important at elevated temperatures, and hot coated surfaces that view each other can exchange radiation. Radiative exchange calculations are usually for surfaces that are opaque, and each surface has a specific radiating temperature. The analysis must be different when some or all of the surfaces have translucent coatings. Some protective coating materials such as zirconia and alumina, are partially transparent to portions of the thermal radiation spectrum. Hence, the radiative exchange process is more complex since radiation from a coated area depends on the temperatures within its coating. These temperatures are unknown, and they depend on the exchange process. The exchange analyzed here is for a parallel-plate enclosure that can have different heating conditions for the internal and external surfaces of each coated wall. Each wall has an opaque outer layer such as a metal plate, and a translucent coating on the inside. The coatings on opposite walls view each other and exchange radiation. An analytical method is developed for obtaining the temperature distribution in each coating and its opaque substrate. Illustrative results are provided for coatings with various optical thicknesses, and are compared with results for opaque coatings. © 1998 Elsevier Science Ltd. All rights reserved.

*Key words:* Thermal barrier coatings; Radiative enclosures; Translucent coatings; Radioactive exchange

---

## Nomenclature

$a_j$  absorption coefficient of each translucent coating ( $j = 1, 2$ ) [ $\text{m}^{-1}$ ]  
 $G$  flux quantity in two-flux method [ $\text{W m}^{-2}$ ]  
 $\tilde{G}$  dimensionless flux quantity,  $\tilde{G} = G/\sigma T_{\text{gi}2}^4$   
 $g$  Green's function for  $\tilde{G}(X)$  in coating  
 $h_{ij}$  convective heat transfer coefficients at inside boundaries (Fig. 1) [ $\text{W m}^{-2} \text{K}^{-1}$ ]  
 $h_{oj}$  convective heat transfer coefficients at outside boundaries (Fig. 1) [ $\text{W m}^{-2} \text{K}^{-1}$ ]  
 $H_j$  dimensionless convection parameter,  $H_j = h_j/\sigma T_{\text{gi}2}^3$   
 $k_c, k_m$  thermal conductivity of coating, and of metal or opaque substrate [ $\text{W m}^{-1} \text{K}^{-1}$ ]  
 $K_j$  extinction coefficients of coatings,  $a_j + \sigma_{sj}$  [ $\text{m}^{-1}$ ]

$N_c, N_w$  conduction–radiation parameters,  $N_c = k_c/\delta_c \sigma T_{\text{gi}2}^3$ ,  $N_w = k_w/\delta_w \sigma T_{\text{gi}2}^3$   
 $m_j$  the quantity  $K_j \delta_{cj} [3(1 - \Omega_j)]^{1/2}$   
 $n_j$  refractive indices of translucent coatings  
 $Pi_j$  the quantity  $2Ri_j/3K_j \delta_{cj}$   
 $Pw_j$  the quantity  $2(2 - \epsilon_{ij})/3K_j \delta_{cj} \epsilon_{ij}$   
 $q$  heat flux [ $\text{W m}^{-2}$ ], dimensionless flux,  $\tilde{q} = q/\sigma T_{\text{gi}2}^4$   
 $q_r$  radiative heat flux [ $\text{W m}^{-2}$ ]  
 $q_r^+, q_r^-$  radiative heat fluxes in positive and negative  $x$  directions [ $\text{W m}^{-2}$ ]  
 $q_{r1}, q_{r2}$  externally incident radiative fluxes (Fig. 1) [ $\text{W m}^{-2}$ ]  
 $q_{\text{tot},j}$  total heat flux by combined conduction and radiation [ $\text{W m}^{-2}$ ]  
 $Ri_j$  the reflectivity ratio,  $(1 + \rho_{ij})/(1 - \rho_{ij})$   
 $Ro_j$  the reflectivity ratio,  $(1 - \rho_{oj})/(1 - \rho_{ij})$   
 $T$  absolute temperature [K]  
 $t$  dimensionless temperature,  $t = T/T_{\text{gi}2}$   
 $T_c, T_w$  temperatures of coating and substrate  
 $T_{\text{gi}1}, T_{\text{gi}2}$  gas temperatures adjacent to boundaries inside

---

\* Corresponding author. Tel.: 001 216 433 5831; fax: 001 216 433 8864; e-mail: robert.siegel@lerc.nasa.gov

enclosure (Fig. 1);  $T_{gi2}$  is used as reference temperature [K]

$T_{go1}, T_{go2}$  gas temperatures on outside of enclosure (Fig. 1) [K]

$T_{s1}, T_{s2}$  temperatures of blackbody surroundings on outside of enclosure (Fig. 1) [K]

$x_j$  coordinate in coating and substrate composite (Fig. 1) [m],  $X_j = x_j/\delta_{cj}$ .

#### Greek symbols

$\delta_{cj}, \delta_{wj}$  thicknesses of translucent coating, and opaque substrate [m]

$\varepsilon_{ij}, \varepsilon_{oj}$  substrate emissivity (in vacuum) at inside and outside boundaries (Fig. 1)

$\kappa_{cj}$  optical thickness of coating,  $(a_j + \sigma_{sj})\delta_{cj} = K_j\delta_{cj}$

$\rho$  diffuse reflectivity

$\sigma$  Stefan–Boltzmann constant [ $\text{W m}^{-2} \text{K}^{-4}$ ]

$\sigma_{sj}$  scattering coefficient in semitransparent coating [ $\text{m}^{-1}$ ]

$\Omega_j$  scattering albedo of coating,  $\Omega_j = \sigma_{sj}/(a_j + \sigma_{sj}) = \sigma_{sj}/K_j$ .

#### Subscripts

c translucent coating

h homogeneous solution of two-flux equation

i, o inside and outside interfaces of exposed surface of coating (Fig. 1); inside and outside surfaces of substrate (Fig. 1)

in incident on coating surface from its surroundings

$j = 1, 2$  two coated walls of the enclosure (Fig. 1)

r radiative

tot total heat flux including radiation, conduction, and convection

w opaque substrate

1, 2 two coated walls of the enclosure (Fig. 1).

## 1. Introduction

For some high temperature applications, thermal barrier coatings can be used on walls to reduce wall temperatures, heat flows, and thermal gradients [1]. Coatings may also be required to protect walls from corrosive environments [2]. At high temperatures, radiative transfer may be important in the heat transfer performance, and if coated surfaces can view each other, they will exchange radiation. In conventional radiative exchange calculations as detailed in textbooks [3], the surfaces are opaque, and each area of a radiative enclosure has single radiating temperature. Some thermal barrier coating materials, however, are partially transparent to thermal radiation [4–6], so the exchange process is complicated by radiation within each coating thickness. The radiation leaving an enclosure area then depends on the temperature distribution within its coating. This distribution is unknown, and depends on the exchange process. Hence, a radiating area with a translucent coating cannot be considered to have a single radiating temperature.

An analytical method is developed here for a parallel-plate enclosure with this type of radiative exchange. As shown in Fig. 1, parallel plates are considered where each wall can be subjected to a different external heating condition, and there is convection in the enclosure by a hot transparent gas. Each enclosure wall has a metal or opaque outer layer, and has a protective translucent

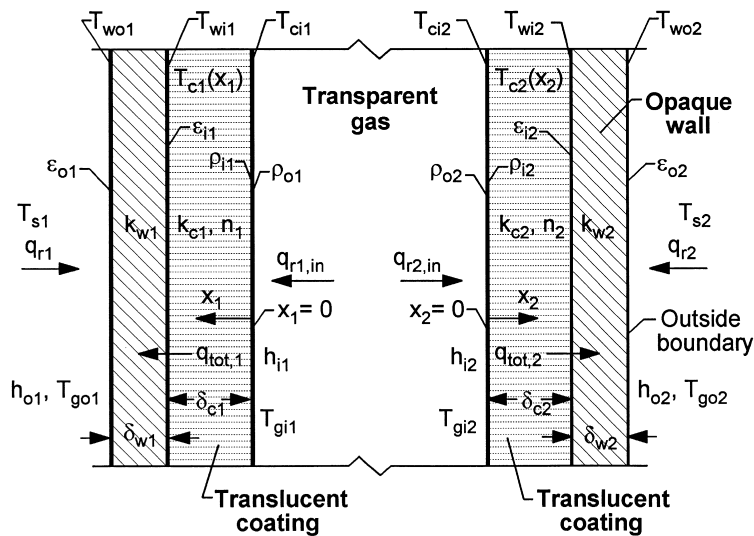


Fig. 1. Geometry and nomenclature for translucent protective coatings on each opaque wall of a parallel-plate enclosure with internal convection and radiation exchange, and convection and radiation at external boundaries.

ceramic coating on the inside of the enclosure. The coated walls view each other and exchange radiation. An absorbing gas in the enclosure would radiate energy and would decrease exchange between the walls, these complications are not considered here. The wall temperatures are assumed to not vary along the length of each wall. The theory is a continuation of the development in [7] where a channel with symmetric convective heating conditions was considered.

Energy transfer computations in a hot translucent coating include heat conduction, internal radiative emission, and radiative transport by the processes of absorption, emission, and scattering. Since combined conduction–radiation calculations using the exact radiative transfer equations can become somewhat complicated as discussed in textbooks such as [3], it is desirable to use simplified methods for analysis if these will yield good results. Some approximate analysis methods were applied in [8] for plane layers of translucent materials with isotropic scattering, and results were compared with solutions where the complete radiative transfer equations were used. It was found that the two-flux method gave accurate results for layers with diffuse boundaries. Diffuse boundaries are a reasonable assumption for thermal barrier and protective coatings since they have a somewhat rough exterior and a granular or columnar structure.

A two-flux method is developed here to obtain temperature distributions in the coated walls of a parallel-plate enclosure. Following the ideas in [9] and [10], a Green's function is derived to provide an analytical solution for the differential equation governing the radiative flux function in the two-flux method. The Green's function includes the enclosure radiative exchange boundary condition. The radiative flux function from the Green's function is incorporated into an iterative solution for the temperature distribution and heat flow in each translucent coating and its opaque substrate, including radiative exchange between the coated surfaces.

Illustrative results are given for temperature distributions in translucent coatings on opaque substrates in an enclosure with convection on the boundaries, and with radiative exchange between coated surfaces. The effects of some parameters are examined, and comparisons are made with temperatures in opaque coatings. The results are for gray coatings, but extensions to include spectral variations can be made as described in [7] and [9].

## 2. Analysis

### 2.1. Energy and two-flux relations

A parallel-plate enclosure, Fig 1, has each opaque wall coated on the inside with a protective coating that is

translucent for thermal radiation. An  $x$ -coordinate starts at the inside surface of each coating and extends outward. Inside the enclosure there is hot transparent gas that provides convection with heat transfer coefficients  $h_{i1}$  and  $h_{i2}$  at the exposed inside boundaries of the protective coatings. The exterior surfaces of the opaque substrates are subject to both convection and radiation. In each translucent coating the total heat flux is the sum of radiation and conduction, and the energy equation in each coating is given by [9],

$$q_{\text{tot},j} = -k_{c,j} \frac{dT_{c,j}(x_j)}{dx_j} + q_{r,j}(x_j) \quad j = 1, 2. \quad (1)$$

In this study the coatings are assumed gray, and  $j = 1$  and  $2$  correspond to the left and right sides of the enclosure in Fig. 1. For steady-state conditions the total heat flux through each composite wall,  $q_{\text{tot},j}$ , is independent of  $x_j$ .

To solve equation (1) for  $T_{c,j}(x_j)$ , a relation is needed for the local radiative flux  $q_{r,j}(x_j)$ . In the two-flux method the  $q_{r,j}(x_j)$  is related to a flux quantity  $G_j(x_j)$  by the relation [8],

$$q_{r,j}(x_j) = -\frac{1}{3(a_j + \sigma_{s,j})} \left. \frac{dG_j}{dx_j} \right|_{x_j} \quad j = 1, 2. \quad (2)$$

The  $G_j(x_j)$  will be obtained by solving an auxiliary equation that will be defined. After substituting equation (2) into equation (1), the result is integrated with respect to  $x_j$  to give a relation for the temperatures in each coating in terms of some quantities that will be determined,

$$T_{c,j}(x_j) = T_{c,i,j} - \frac{1}{k_{c,j}} \left[ q_{\text{tot},j} x_j - \frac{G_j(0) - G_j(x_j)}{3(a_j + \sigma_{s,j})} \right] \quad j = 1, 2. \quad (3)$$

To evaluate the  $T_{c,j}(x_j)$  in each translucent coating, the  $T_{c,i,j}$ ,  $q_{\text{tot},j}$ , and  $G_j(x_j)$  must be obtained as will be described.

From the two-flux method, the flux quantity  $G_j(x_j)$  is found by solving a differential equation that includes the local blackbody emission and the scattering albedo [9],

$$\begin{aligned} \frac{d^2 G_j(x_j)}{dx_j^2} - 3K_j^2(1 - \Omega_j)G_j(x_j) \\ = -3K_j^2(1 - \Omega_j)4n_j^2 \sigma T_{c,j}^4(x_j) \quad j = 1, 2. \end{aligned} \quad (4)$$

The  $T_{c,j}(x_j)$  in each translucent coating will be evaluated by iteration because the radiative exchange depends on all of the unknown coating temperature distributions.

To solve the second-order equation, equation (4), two boundary conditions are required. The general boundary condition for  $G_j(0)$  at the translucent coating boundary  $x_j = 0$  is as follows [6], when it is subjected to an incident radiative flux  $q_{r,j,\text{in}}$  from its surroundings,

$$G_j(0) - \frac{2}{3K_j} \frac{1 + \rho_{i,j}}{1 - \rho_{i,j}} \left. \frac{dG_j}{dx_j} \right|_{x_j=0} = 4 \frac{1 - \rho_{o,j}}{1 - \rho_{i,j}} q_{r,j,\text{in}} \quad j = 1, 2. \quad (5)$$

The incident flux  $q_{rj,in}$  is unknown as it arises primarily from radiation leaving the opposite coated wall, and it depends on the unknown temperature distributions in the coatings that are to be obtained by the solution.

The second boundary condition for solving equation (4) is at the coating–substrate interface,  $x_j = \delta_{cj}$ ; this is given by [6],

$$G_f(\delta_{cj}) + \frac{2}{3K_j} \frac{2 - \varepsilon_{ij}}{\varepsilon_{ij}} \left. \frac{dG_f}{dx_j} \right|_{x_j=\delta_{cj}} = 4n_j^2 \sigma T_{wij}^4 \quad j = 1, 2. \quad (6)$$

Equation (4), with the boundary conditions equations (5) and (6), can be solved for  $G_f(x_j)$  in a convenient form by obtaining a Green's function. From the analysis in [9] for a translucent layer on an opaque substrate, the Green's function is in two parts and has the following dimensionless form with  $X_j = x_j/\delta_{cj}$ ,

$$g_f(X_j, \xi_j) = \left\{ \frac{\sinh m_j(1 - \xi_j) + Pw_j m_j \cosh m_j(1 - \xi_j)}{(1 + Pi_j Pw_j m_j^2) \sinh m_j + (Pw_j + Pi_j) m_j \cosh m_j} \right\} \times [\sinh m_j X_j + Pi_j m_j \cosh m_j X_j] \quad 0 \leq X_j < \xi_j \quad (7a)$$

$$g_f(X_j, \xi_j) = \left\{ \frac{\sinh m_j \xi_j + Pi_j m_j \cosh m_j \xi_j}{(1 + Pi_j Pw_j m_j^2) \sinh m_j + (Pw_j + Pi_j) m_j \cosh m_j} \right\} \times [\sinh m_j(1 - X_j) + Pi_j m_j \cosh m_j(1 - X_j)]. \quad \xi_j < X_j \leq 1 \quad (7b)$$

The  $g_f(X_j, \xi_j)$  in equation (7) is used to obtain the effect of the nonhomogeneous term in equation (4) when computing the dimensionless  $\tilde{G}_f(X_j)$ . To obtain the complete solution for  $\tilde{G}_f(X_j)$ , the solution for the homogeneous part of equation (4) is also needed. Following the procedure in [10] the general homogeneous solution is

$$\tilde{G}_{hj}(X_j) = A_j \sinh m_j X_j + B_j \cosh m_j X_j \quad j = 1, 2. \quad (8a)$$

The boundary conditions equations (5) and (6) are applied to give relations for  $B_j$  and  $A_j$ ,

$$B_j = 4 \frac{Pi_j m_j n_j^2 t_{wij}^4 + Ro_j \tilde{q}_{rj,in} (\sinh m_j + Pw_j m_j \cosh m_j)}{(1 + Pi_j Pw_j m_j^2) \sinh m_j + (Pw_j + Pi_j) m_j \cosh m_j} \quad (8b)$$

$$A_j = \frac{B_j - 4Ro_j \tilde{q}_{rj,in}}{Pi_j m_j} \quad (8c)$$

The  $t_{wij}$  and  $\tilde{q}_{rj,in}$  must be determined during the solution.

By adding  $\tilde{G}_{hj}(X_j)$  and the nonhomogeneous solution obtained with  $g_f(X_j, \xi_j)$ , the solution of equation (4) in dimensionless form is

$$\tilde{G}_f(X_j) = \tilde{G}_{hj}(X_j) + 4m_j n_j^2 \int_0^1 g_f(X_j, \xi_j) t_{cj}^4(\xi_j) d\xi_j. \quad (9)$$

Now that a relation for  $\tilde{G}_f(X_j)$  has been developed, relations will be found for the surface temperature  $T_{cij}$  and total heat flux  $q_{tot,j}$  that are needed to evaluate equation (3). These are obtained by writing total energy flux relations for each coating and its opaque substrate. At the exposed surface of a coating inside the enclosure, the total heat flux within the coating is by radiation and conduction, equation (1). For a gray translucent coating there are no opaque spectral regions. Conduction at the boundary is then equal to the external convection as there is no radiant absorption at the plane of the translucent surface, and by use of equations (1) and (2) the result for  $q_{tot,j}$  is,

$$q_{tot,j} = h_{ij}(T_{gij} - T_{cij}) - \frac{1}{3(a_j + \sigma_{sj})} \left. \frac{dG_f}{dx_j} \right|_{x_j=0}. \quad (10a)$$

In the translucent coating, by use of equation (3) evaluated at the coating–substrate interface  $x_j = \delta_{cj}$ ,

$$q_{tot,j} = \frac{k_{cj}}{\delta_{cj}} (T_{cij} - T_{wij}) + \frac{G_f(0) - G_f(\delta_{cj})}{3(a_j + \sigma_{sj})\delta_{cj}}. \quad (10b)$$

At the interface of the translucent coating and the opaque substrate, continuity of temperature gives  $T_{cj}(\delta_{cj}) = T_{wj}(\delta_{cj})$ . In the opaque wall, heat is transferred only by conduction so,

$$q_{tot,j} = \frac{k_{wj}}{\delta_{wj}} (T_{wij} - T_{woj}). \quad (10c)$$

At the outside of the substrate, heat flow is by convection of the external gas, and there is radiative exchange that is assumed to be to a large surrounding environment with an effective blackbody temperature  $T_{sj}$ . Then,

$$q_{tot,j} = h_{oj}(T_{woj} - T_{goj}) + \varepsilon_{oj} \sigma (T_{woj}^4 - T_{sj}^4). \quad (10d)$$

Equations (10a) to (10d) are solved numerically for  $T_{cij}$ ,  $T_{wij}$ ,  $T_{woj}$ , and  $q_{tot,j}$ . The temperature distribution in the translucent coating is then evaluated from equation (3) using  $G_f(x_j)$  from equation (9). An iterative method is used to obtain the converged solution for  $T_{cj}(x_j)$  and  $T_{wj}(x_j)$  as will be described.

A way must be provided for determining the  $q_{rj,in}$  as needed for equation (8b). For each coating  $q_{rj,in}$  depends partly on the radiation leaving the other coating. From equations (10a) and (2),

$$q_{rj}(0) = q_{tot,j} - h_{ij}(T_{gij} - T_{cij}) \quad (11a)$$

and from the basic two-flux relations, the radiative flux in the negative  $x_j$  direction at  $x_j = 0$  inside each coating is [8],

$$q_{rj}^-(0) = \frac{1}{2} \left[ \frac{G_f(0)}{2} - q_{rj}(0) \right]. \quad (11b)$$

Two relations for the  $q_{rj,in}$  are now written where each has a transmitted and reflected component (Fig. 1),

$$q_{r1,in} = (1 - \rho_{i2})q_{r2}^-(0) + \rho_{o2}q_{r2,in}$$

$$q_{r2,in} = (1 - \rho_{i1})q_{r1}^-(0) + \rho_{o1}q_{r1,in}$$

These two relations are solved for  $q_{r1,in}$  and  $q_{r2,in}$  to give,

$$q_{r1,in} = \frac{1 - \rho_{i2}}{1 - \rho_{o1}\rho_{o2}} q_{r2}^-(0) + \frac{\rho_{o2}(1 - \rho_{i1})}{1 - \rho_{o1}\rho_{o2}} q_{r1}^-(0) \quad (11c)$$

$$q_{r2,in} = \frac{1 - \rho_{i1}}{1 - \rho_{o2}\rho_{o1}} q_{r1}^-(0) + \frac{\rho_{o1}(1 - \rho_{i2})}{1 - \rho_{o2}\rho_{o1}} q_{r2}^-(0). \quad (11d)$$

## 2.2. Relations for temperatures in opaque layers

The limiting solution where the protective coatings inside the enclosure are opaque, is used for comparison with results for translucent coatings, and for starting the iterative calculations. The opaque solution is found by solving the following equations for total heat flux written for each coated substrate. At the external boundary of substrate 1,

$$q_{tot,1} = h_{o1}(T_{wo1} - T_{go1}) + \varepsilon_{o1}\sigma(T_{wo1}^4 - T_{s1}^4). \quad (12a)$$

In the composite opaque coating and substrate, the heat transfer by conduction is,

$$q_{tot,1} = \frac{T_{ci1} - T_{wo1}}{\frac{\delta_{c1}}{k_{c1}} + \frac{\delta_{w1}}{k_{w1}}}. \quad (12b)$$

Convection and radiative exchange at the coating surface, including radiative exchange between the two coating surfaces inside the enclosure, gives for coating 1,

$$q_{tot,1} = h_{i1}(T_{gi1} - T_{ci1}) + \frac{(1 - \rho_{o1})(1 - \rho_{o2})}{1 - \rho_{o1}\rho_{o2}} \sigma(T_{ci2}^4 - T_{ci1}^4). \quad (12c)$$

Similarly for coating and substrate 2, the equations are,

$$q_{tot,2} = h_{i2}(T_{gi2} - T_{ci2}) + \frac{(1 - \rho_{o2})(1 - \rho_{o1})}{1 - \rho_{o2}\rho_{o1}} \sigma(T_{ci1}^4 - T_{ci2}^4) \quad (12d)$$

$$q_{tot,2} = \frac{T_{ci2} - T_{wo2}}{\frac{\delta_{c2}}{k_{c2}} + \frac{\delta_{w2}}{k_{w2}}} \quad (12e)$$

$$q_{tot,2} = h_{o2}(T_{wo2} - T_{go2}) + \varepsilon_{o2}\sigma(T_{wo2}^4 - T_{s2}^4). \quad (12f)$$

Equations (12a)–(12f) are solved numerically for  $T_{cij}$ ,  $T_{woj}$ , and  $q_{tot,j}$ . Using heat conduction relations, the temperature distribution in each coating and substrate is then obtained. From the radiative exchange relations between the inside surfaces of the opaque coatings,

$$q_{r1,in} = \frac{1}{1 - \rho_{o1}\rho_{o2}} [(1 - \rho_{o2})\sigma T_{ci2}^4 + \rho_{o2}(1 - \rho_{o1})\sigma T_{ci1}^4] \quad (13a)$$

$$q_{r2,in} = \frac{1}{1 - \rho_{o2}\rho_{o1}} [(1 - \rho_{o1})\sigma T_{ci1}^4 + \rho_{o1}(1 - \rho_{o2})\sigma T_{ci2}^4]. \quad (13b)$$

These  $q_{rj,in}$  relations are needed for starting the iterative solution.

## 2.3. Iterative solution method

The relations were placed in dimensionless form using the quantities in the Nomenclature, and an iterative solution was used to obtain the temperature distribution in each coating and substrate. The method provided good convergence for all calculations that were made, and less than 50 iterations were usually required to reach convergence to five figures in the dimensionless temperatures  $t_c(X_j) = T_c(x_j)/T_{gi2}$ , and  $t_w(X_j)$ . To start the iteration the opaque heat conduction solution from equation (12) was used as a first guess for  $t_c(X_j)$ , and the opaque coating temperatures were also used in equations (13) to obtain a first guess for  $q_{r1,in}$  and  $q_{r2,in}$ . Then using the specified radiation properties for the gray coatings, the Green's function was evaluated for each coating from equation (7). The homogeneous solution for each coating was evaluated from equation (8) where  $t_{wij}$  and  $\tilde{q}_{rj,in}$  were evaluated from the opaque solution and equation (13). Evaluating equation (9) then gave  $\tilde{G}_j(X_j)$  for each coating; double precision was used for the integrations involving Green's functions. Equations (10a)–(10d) were then solved for  $t_{cij}$  and  $\tilde{q}_{tot,j}$  and equation (3) was used to evaluate new  $t_c(X_j)$  for each coating. A damping factor of usually 0.025–0.05 was used to decrease changes in  $t_c(X_j)$  between successive iterations; this was required for stability. This gave the  $t_c(X_j)$  to start the next iteration using equations (8) and (9). Equations (11a)–(11d) were then used to obtain  $q_{r1,in}$  and  $q_{r2,in}$  that are needed during the next iteration. The procedure was continued until  $t_c(X_j)$  converged for both coatings.

## 3. Results and discussion

There are many parameters such as optical thicknesses, convection coefficients, thermal conductivities, and refractive indices, that determine the heat transfer behavior in an enclosure with translucent protective coatings on its interior boundaries. The purpose of this work is to develop a solution method, and with the relations provided here, temperature distributions in the coatings can be evaluated for a variety of conditions. For a discussion of reasonable length, it is not possible to show

the effect of many of the parameters in detail. Hence, the results given here are intended only to illustrate some of the thermal behavior of translucent coatings on the inside of opaque walls of a parallel-plate enclosure. Each coating has convection at its surface by a hot transparent gas, and temperatures are high enough to provide significant radiation effects.

### 3.1. Temperature distributions in walls with translucent thermal barrier coatings

The results in this section are for coatings that each provide a thermal barrier to reduce temperatures in its substrate. Each substrate is cooled on the outside by convection and radiation, and each coating is being heated at its exposed surface by convection of a transparent gas. The heat flow through each coated wall is outward through the substrate so temperatures in each substrate are reduced by its coating. The two parts of Fig. 2 have the same boundary conditions, but have different refractive indices,  $n = 1$  and  $2$  in parts (a) and (b). The coatings are gray, there is no scattering, and the optical thickness of each coating is  $\kappa_{c_j} = 1$ . The substrates are opaque, and the solid lines show temperature distributions when the coatings are translucent, and are compared with the dashed lines that are for opaque coatings. The sets of curves marked 'A' are for the same boundary conditions on both walls. The results by the present method agree with those in [7] where the symmetric case was analyzed, as an important special case for gas flow in a channel, by applying symmetric conditions and evaluating the applicable Green's function for the two-flux function. The conduction and convection parameters for Fig. 2 are in the figure caption. The  $k/\delta$  in the substrate is 10 times larger than in the coating that is more of an insulating material. For the parameters chosen for curves 'A' in Fig. 2(a), there is a considerable radiation effect in increasing substrate temperatures, as is evident by comparing temperatures for a translucent coating (solid lines) with those for an opaque coating (dashed lines). The translucence of the coating degrades its performance as a thermal barrier coating, so the substrate temperatures are higher than when the coating is opaque. The temperature distributions in the translucent coating have an 'S' shape that is typical of a layer with heat flow in one direction by combined radiation and conduction.

For the curves marked 'B' in Fig. 2(a), the gas temperature for convective heating of the coating on the left side of the enclosure (coating 1), was increased to twice that for coating 2 on the right side. The temperature distribution in coating 1 still has an 'S' shape as energy is flowing from the interior surface at  $x_1 = 0$ , through the coating and substrate to the cooled exterior boundary at  $x_1/\delta_{c_1} = 2$ . The hot coating on the left side is radiating to the cooler coating on the right, and energy is being

absorbed within coating 2. This changes the shape of the temperature distribution on the right side. The interior of the coating is raised above the gas temperature at  $x_2 = 0$  that is  $t_{g_{i2}} = 1$ , so the gas is now convectively cooling the coating that is being heated by radiation. This results in a positive temperature gradient near the boundary  $x_2 = 0$ .

The curves marked 'C' show the effect of increasing the internal convective heat transfer coefficients  $h_{i1}$  and  $h_{i2}$  by a factor of 10 while keeping the gas temperatures the same as for 'B'. The temperature at the interior surface  $x_1 = 0$  of coating 1 then rises toward its possible upper limit of  $t_{g_{i1}} = 2$  that would occur if  $h_{i1}$  became infinite. Similarly on the right side, the surface temperature at  $x_2 = 0$  is reduced to near 1 which is the value of  $t_{g_{i2}}$ . The larger difference between the coating temperatures increases the radiative transfer from coating 1 to coating 2. Internal absorption raises temperatures within the coating on the right side, and the convective cooling effect near its boundary increases, producing a large temperature gradient near  $x_2 = 0$ . For coating 2, internal radiative heating with cooling at both boundaries produces the maximum temperature inside the coating.

The purpose of Fig. 2(b) is to illustrate the effect of the coating refractive indices, that have been increased to  $n_j = 2$  compared with  $n_j = 1$  in Fig. 2(a). A refractive index of  $n_j = 2$  is typical of some ceramic materials used for thermal barrier coatings. The results are similar to Fig. 2(a), but the increased  $n_j$  has made the temperature distributions in the coatings more uniform except near the exposed boundaries where convection produces large gradients. For  $n_j = 2$  the reflectivity of the coating surface was obtained using the Fresnel relations [3] and assuming diffuse surfaces. Reflectivity values are in the figure caption.

The results in Fig. 3 with  $n_j = 1$  are a further development of those in Fig. 2(a) and are for the same boundary conditions and refractive index. The convective parameters in Fig. 3 are the same as for curves 'C' in Fig. 2(a), and these temperature distributions are repeated on Fig. 3 as they provide a comparison where there is no scattering. The purpose of Fig. 3 is to demonstrate the effect of adding scattering while keeping absorption the same. The optical thickness for absorption is  $a_j\delta_{c_j} = 1$  for all of the translucent layers, while the coating optical thickness is increased by adding scattering to give the values shown for  $\kappa_{c_j} = (a_j + \sigma_{s_j})\delta_{c_j} > 1$ . The results for  $\kappa_{c_j} = 1$  are the same as curves 'C' in Fig. 2(a). The effect of additional scattering is to provide shielding of the substrate from radiative effects, and temperatures in the substrates are reduced. For an optical thickness of  $\kappa_{c_j} = 100$  the distributions are approaching the opaque limit although there is only a small amount of absorption. This is the behavior in the diffusion limit where scattering is grouped together with absorption and the results depend only on the extinction coefficient.

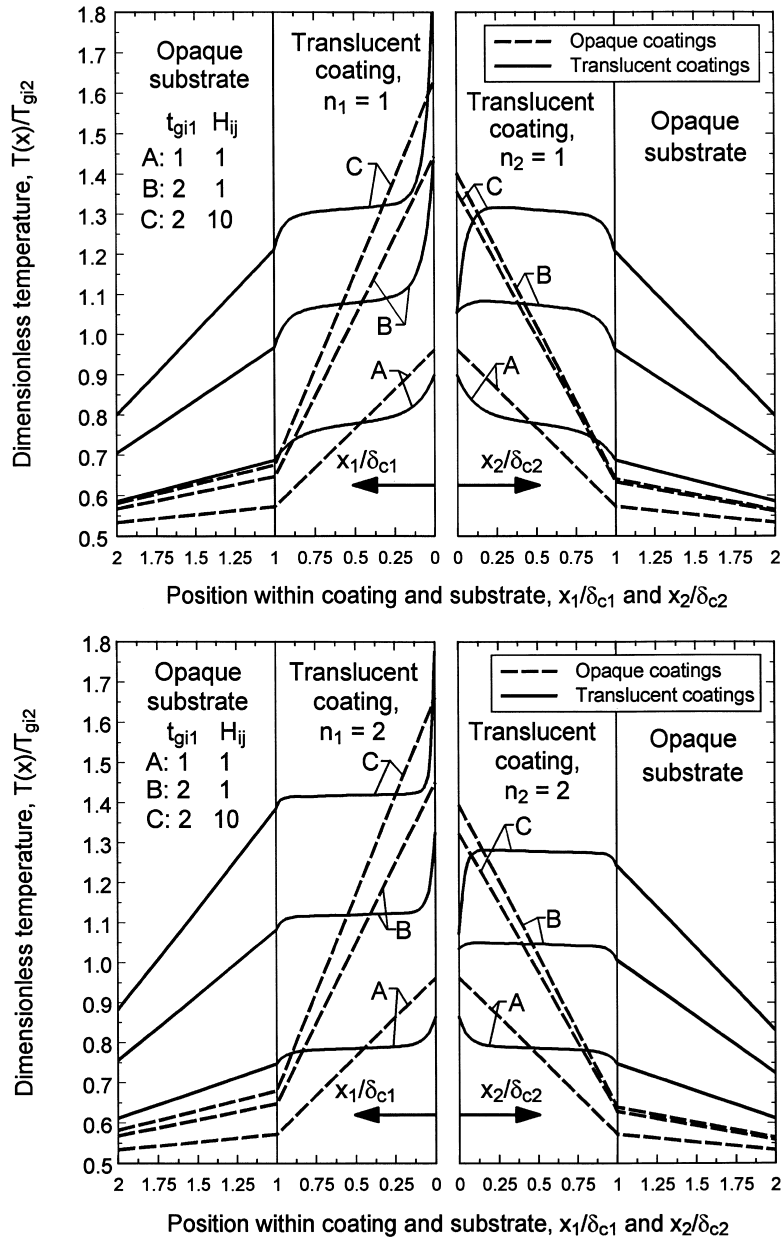


Fig. 2. Effect of various heating and cooling conditions on temperature distributions in translucent thermal barrier coatings on opaque walls of a parallel-plate enclosure. Parameters:  $\kappa_{cj} = 1, t_{gi2} = 1, t_{goj} = 0.5, H_{oj} = 1, N_{cj} = 0.1, N_{wj} = 1, \Omega_j = 0, \epsilon_{ij} = \epsilon_{oj} = 0.3$ . (a) Coating refractive indices,  $n_j = 1, \rho_{oj} = \rho_{ij} = 0$ . (b) Coating refractive indices,  $n_j = 2, \rho_{oj} = 0.16060, \rho_{ij} = 0.79015$ .

3.2. Temperature distributions in walls with translucent protective coatings

In Fig. 4 the coatings in the enclosure are for protection of the substrates from a corrosive environment. The coated wall on the left side is being heated on the outside and the heat flow is in the direction from the substrate into the coating, so the coating is not acting as a thermal

barrier. Going from left to right in Fig. 1, the gas temperatures for Fig. 4 are  $t_{go1} = 2, t_{gi1} = t_{gi2} = 1,$  and  $t_{go2} = 0.5$ , so energy is flowing from left to right through the enclosure. The dashed lines are for opaque coatings with only heat conduction in the coated walls. For opaque coatings there is radiation at the surfaces, so radiation is exchanged across the enclosure between the coating surfaces. For the parameters in Fig. 4(a) the

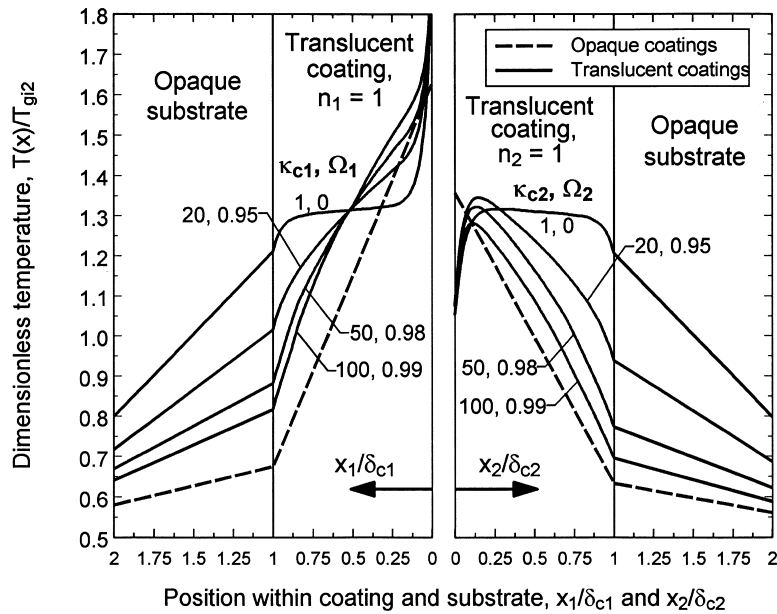


Fig. 3. Effect of scattering on temperature distributions in translucent thermal barrier coatings where both walls are cooled on the outside,  $a_j \delta_{c_j} = 1$ ,  $\sigma_j \delta_{c_j} = 0$ , 19, 49, 99 so that  $(a_j + \sigma_j) \delta_{c_j} = \kappa_{c_j} = 1, 20, 50, 100$ . Parameters:  $t_{gi1} = 2$ ,  $t_{gi2} = 1$ ,  $t_{goj} = 0.5$ ,  $H_{oj} = 1$ ,  $H_{ij} = 10$ ,  $N_{c_j} = 0.1$ ,  $N_{w_j} = 1$ ,  $n_j = 1$ ,  $\varepsilon_{ij} = \varepsilon_{oj} = 0.3$ .

temperature decrease is small between the surfaces of coatings 1 and 2. However, there is significant radiative transfer from coating 1 to coating 2 as evidenced by the shapes of the temperature distributions in translucent coatings for  $\kappa_{c_j} = 1$ . In coating 2 the temperatures are highest away from the boundary with dimensionless temperatures larger than one, and there is cooling by convection at  $x_2 = 0$  by gas at  $t_{gi2} = 1$ . The temperature at the boundary is thus lower than in the interior as a result of internal heating by radiation, with convective cooling at the boundary. As the optical thickness is increased, radiative penetration into coating 2 is only significant near  $x_2 = 0$ , and there is only a small region where the interior temperatures are larger than at the boundary. In Fig. 4(a) the optical thicknesses extend to 50, and as the optical thickness increases, the temperatures are approaching the opaque limit. For optical thicknesses greater than about 20, the analysis in [7] shows that a diffusion approximation gives reasonable results, and is quite convenient to use. For spectral calculations the application of the diffusion equation is provided in [8].

The effect of increasing the coating indices of refraction is in Fig. 4(b), where  $n_j = 2$  as compared with  $n_j = 1$  in Fig. 4(a). The general trends of the temperature distributions relative to each other are the same, but there are some significant differences. For an increased refractive index, the temperatures are more uniform in the interior portion of each coating away from the boundaries. This is probably the result of increased internal

emission produced by the  $n^2$  factor in the local radiative emission, and the resulting increased reflections at the boundaries by total internal reflection, that helps distribute energy more uniformly throughout each coating. This behavior also tends to reduce the rate of approach toward the opaque limit with increasing coating optical thickness.

In Fig. 4, the gas temperatures inside the enclosure that provide convection at the coating boundaries are equal,  $t_{gi1} = t_{gi2} = 1$ . To show the effect of a larger radiation transfer between the coatings, the gas temperature adjacent to coating 1 is increased in Fig. 5 to  $t_{gi1} = 2$ , while at the surface of coating 2 the temperature is unchanged,  $t_{gi2} = 1$ . The refractive index in Fig. 5 is  $n_j = 1$ , so comparisons are made with Fig. 4(a). For coating 1, the shapes of the temperature profiles near the boundary  $x_1 = 0$  have changed. The temperatures now increase approaching the boundary from the interior, in contrast to temperatures decreasing adjacent to the boundary in Fig. 4(a). This is the result of heat loss from the interior of coating 1 by radiative transfer to coating 2. This reduces temperatures within coating 1, but its temperatures are increased near the boundary by convective heating by the gas at  $t_{gi1} = 2$ . Consider the results for an optical thickness of  $\kappa_{c_j} = 1$ , where there is a pronounced radiation effect. Coating 1 is being heated by conduction through the opaque substrate at  $x_1 = \delta_{c1}$ , and by convection at  $x_1 = 0$ , and its interior is cooling by radiative loss. The result is a lower temperature region in the interior of the

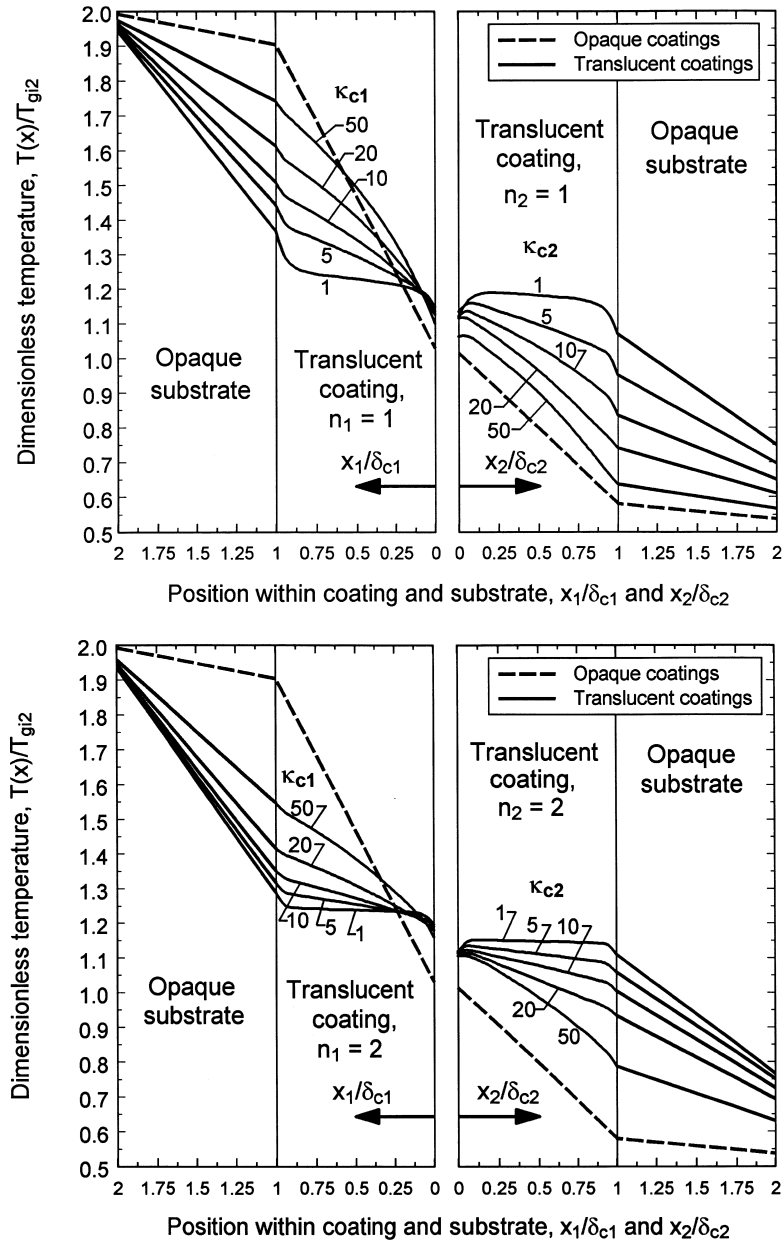


Fig. 4. Temperature distributions in translucent protective coatings with various optical thicknesses on opaque walls of a parallel-plate enclosure, with one wall heated and the other cooled. Parameters:  $t_{gij} = 1$ ,  $t_{g01} = 2$ ,  $t_{g02} = 0.5$ ,  $H_{oj} = H_{ij} = 1$ ,  $N_{cj} = 0.1$ ,  $N_{wj} = 1$ ,  $\Omega_j = 0$ ,  $\epsilon_{ij} = \epsilon_{oj} = 0.3$ . (a) Coating refractive indices,  $n_j = 1$ ,  $\rho_{oj} = \rho_{ij} = 0$ . (b) Coating refractive indices,  $n_j = 2$ ,  $\rho_{oj} = 0.16060$ ,  $\rho_{ij} = 0.79015$ .

coating. In coating 2 the situation is the opposite. Here there is cooling at  $x_2 = \delta_{c2}$  by conduction into the substrate, and cooling by convection at  $x_2 = 0$ . The interior, however, is being heated by radiation from coating 1, so its temperatures are higher than those at the boundaries. Coating 1 has radiative cooling, while coating 2 has radiative heating. For increased optical thicknesses these effects are diminished by having less radiative penetration

within each coating, but the behavior remains the same near the boundaries  $x_j = 0$ .

The results in Fig. 6 are a further development of those in Fig. 5, and are for the same boundary conditions. The refractive index in Fig. 6(a) is  $n_j = 1$ ; this value and some of the optical thicknesses are the same as in Fig. 5. The new parameter in Fig. 6 is the effect of scattering, since the results in Figs 4 and 5 are without scattering. The

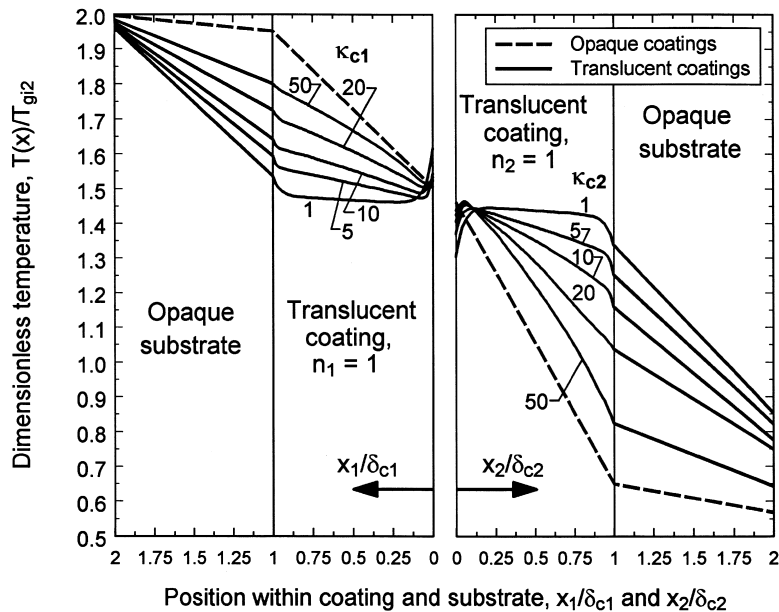


Fig. 5. Effect of unequal gas temperatures at the interior boundaries of two coated walls for translucent protective coatings with various optical thicknesses on opaque walls of a parallel-plate enclosure, with one wall heated and the other cooled. Parameters:  $t_{g11} = 2$ ,  $t_{g12} = 1$ ,  $t_{g01} = 2$ ,  $t_{g02} = 0.5$ ,  $H_{oj} = H_{ij} = 1$ ,  $N_{cj} = 0.1$ ,  $N_{wj} = 1$ ,  $n_j = 1$ ,  $\Omega_j = 0$ ,  $\epsilon_{ij} = \epsilon_{oj} = 0.3$ .

optical thickness for absorption is kept the same in Fig. 6 for all of the translucent coatings,  $a_j \delta_{cj} = 1$ , while the optical thickness is increased by adding scattering to give the values shown for  $\kappa_{cj} = (a_j + \sigma_{sj}) \delta_{cj} > 1$ . The results for  $\kappa_{cj} = 1$  in Fig. 6(a) are the same as in Fig. 5. The effect of increasing the optical thickness with scattering is found to be similar to that without scattering, where the optical thickness is increased by additional absorption as in Fig. 5. For an optical thickness of  $\kappa_{cj} = 100$  in Fig. 6(a) the temperatures are approaching the opaque limit although there is only a small amount of absorption. This corresponds to the behavior in the diffusion limit where scattering combines with absorption and temperatures depend only on the extinction coefficient  $K_j = a_j + \sigma_{sj}$ .

In Fig. 6(b) the refractive index is increased to  $n_j = 2$  in both translucent coatings. The effects are similar to what was discussed for Figs 2 and 4. Increasing  $n_j$  results in less curvature in the central portion of the temperature profiles in a translucent layer. As the optical thickness is increased, the approach toward the opaque limit is at a lower rate than for  $n_j = 1$ . These effects on temperature distributions are significant for ceramic coatings, since a material such as zirconia can have a refractive index of  $n \approx 2$ .

#### 4. Concluding remarks

A combined analytical and numerical iterative method has been developed to determine wall temperature dis-

tributions for a parallel-plate enclosure with walls having translucent protective coatings. This is of interest for operation of heat transfer devices at elevated temperatures to increase thermal efficiency. It may be necessary to use ceramic coatings to protect structural materials from high temperature gases or a corrosive environment. The thermal behavior of translucent protective coatings on the walls of an enclosure is considered here. Some coating materials are translucent for thermal radiation at some radiation frequencies, such as zirconia that is in common use. At elevated temperatures, if several coated walls are present, there is significant radiative exchange between them. In usual radiative exchange calculations the surfaces are opaque, but for this analysis each surface has a translucent coating that has a temperature distribution within its thickness. The temperature distributions in the coatings and in the metal or other opaque substrates, depend on the radiative exchange. However, the exchange depends on the internal temperatures of the coatings that are unknown. A method of analysis was developed to obtain coating and substrate temperature distributions for an enclosure of two parallel plates, heated or cooled by radiation and by convection of a nonradiating gas. The radiative transfer in the coatings, including exchange with the other coated surface, was developed using the two-flux equations. The solution used a Green's function that incorporated the radiative exchange boundary conditions. Illustrative results are provided that show how radiative exchange between surfaces with translucent coatings influences the temperature

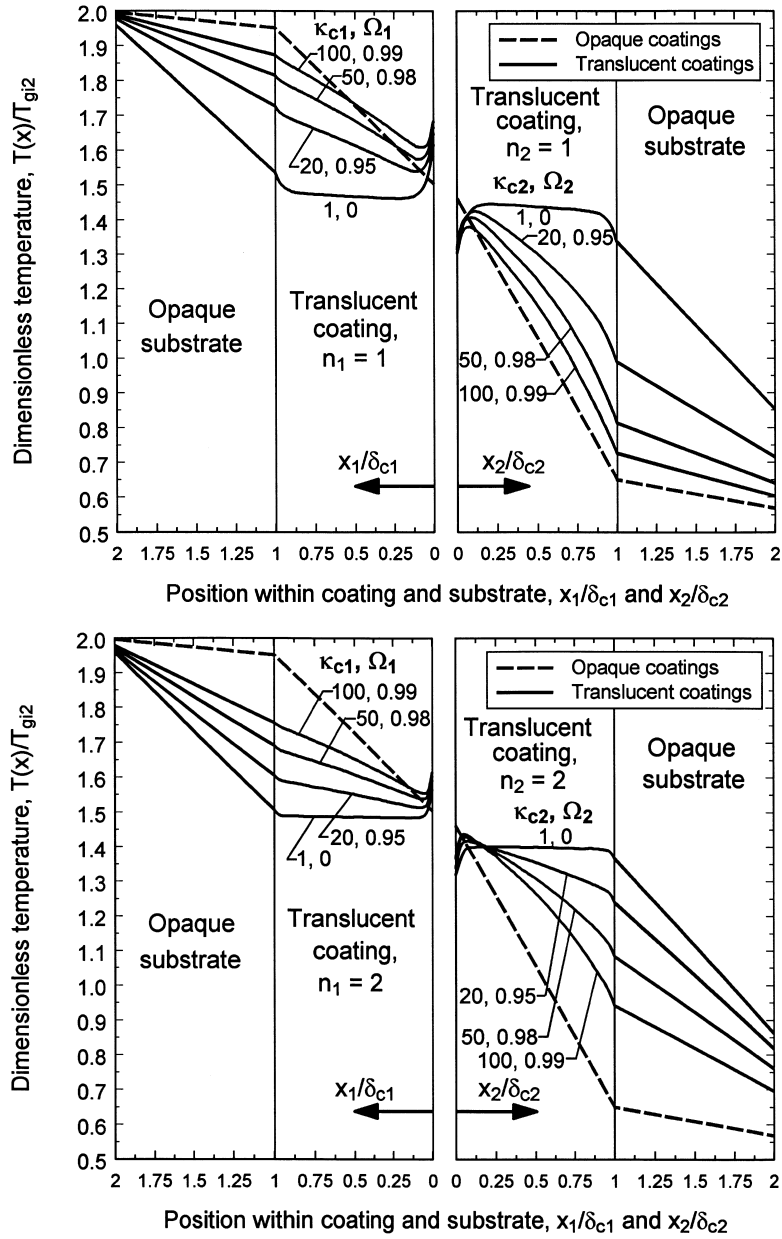


Fig. 6. Effect of scattering on temperature distributions in translucent protective coatings where one wall is heated while the other is cooled,  $a_j \delta_{cj} = 1$ ,  $\sigma_{sj} \delta_{cj} = 0, 19, 49, 99$  so that  $(a_j + \sigma_{sj}) \delta_{cj} = \kappa_{cj} = 1, 20, 50, 100$ . Parameters:  $t_{gi1} = 2$ ,  $t_{gi2} = 1$ ,  $t_{go1} = 2$ ,  $t_{go2} = 0.5$ ,  $H_{oj} = H_{ij} = 1$ ,  $N_{cj} = 0.1$ ,  $N_{wj} = 1$ ,  $\epsilon_{ij} = \epsilon_{oj} = 0.3$ . (a) Coating refractive indices,  $n_j = 1$ ,  $\rho_{oj} = \rho_{ij} = 0$ . (b) Coating refractive indices,  $n_j = 2$ ,  $\rho_{oj} = 0.16060$ ,  $\rho_{ij} = 0.79015$ .

distributions within the coatings. Some of the results are for thermal barrier coatings where each coating is exposed to hot gas and the coating protects its substrate that is being cooled. Other results are for coatings used for protection from a corrosive environment, and in this instance the substrate may be higher in temperature than

the coating depending on the heating conditions. Radiative heating of a coating can provide maximum temperatures within the coating if its boundaries are being cooled by convection or conduction. A coating that is heated at its boundaries by convection or conduction may be cooled by radiation to an adjacent coated wall at

lower temperature; the minimum temperature can then be within the coating. An increased refractive index as is typical of ceramic coatings, tends to reduce curvature of the temperature distributions in the central portion of a coating. It also decreases the approach to the opaque limit as the coating optical thickness is increased.

## References

- [1] Kh.G. Schmitt-Thomas, U. Dietl, H. Haindl, New developments in thermal barrier coatings (TBC) for gas turbine use, *Industrial Ceramics* 16 (1996) 195–198.
- [2] P. Ramaswamy, S. Seetharamu, K.B.R. Varma, K.J. Rao,  $\text{Al}_2\text{O}_3\text{-ZrO}_2$  composite coatings for thermal barrier applications, *Composites Science and Technology* 57 (1997) 81–89.
- [3] R. Siegel, J.R. Howell, *Thermal Radiation Heat Transfer*, 3rd ed., Hemisphere, Washington D.C., 1992, Chap. 4, 7 and 14.
- [4] S. Wahiduzzaman, T. Morel, Effect of Translucence of Engineering Ceramics on Heat Transfer in Diesel Engines, Oak Ridge National Laboratory Report ORNL/Sub/88-22042/2, Oak Ridge, TN, April 1992.
- [5] L.K. Matthews, R. Viskanta, F.P. Incropera, Combined conduction and radiation heat transfer in porous materials heated by intense solar radiation, *Journal of Solar Energy Engineering* 107 (1985) 29–34.
- [6] R. Siegel, Internal radiation effects in zirconia thermal barrier coatings, *Journal of Thermophysics and Heat Transfer* 10 (1996) 707–709.
- [7] R. Siegel, Temperature distributions in channel walls with translucent thermal barrier coatings, *Journal of Thermophysics and Heat Transfer* 12 (1998) 289–296.
- [8] R. Siegel and C.M. Spuckler, Approximate solution methods for spectral radiative transfer in high refractive index layers, *International Journal of Heat and Mass Transfer* 37 (suppl. 1) (1994) 403–413.
- [9] R. Siegel, Green's function to determine temperature distribution in a semitransparent thermal barrier coating, *Journal of Thermophysics and Heat Transfer* 11 (1997) 315–318.
- [10] R. Siegel, Two-flux and Green's function method for transient radiative transfer in a semitransparent layer, *Proceedings of the First International Symposium on Radiative Heat Transfer*, Kuşadası, Turkey, Radiative Transfer—I, Begell House, New York, 1996, pp. 473–487.